Published in final edited form as:
Stem Cells. 2014 October ; 32(10): 2767–2779. doi:10.1002/stem.1758.

sdf1 Expression Reveals a Source of Perivascular-Derived Mesenchymal Stem Cells in Zebrafish

Troy C. Lund[1], **Xiaobai Patrinostro**[1], **Ashley C. Kramer**[1], **Paul Stadem**[1], **LeeAnn Higgins**[2], **Todd W. Markowski**[2], **Matt S. Wroblewski**[2], **Diane S. Lidke**[3], **Jakub Tolar**[1,*], and **Bruce R. Blazar**[1,*]

[1]University of Minnesota, Division of Pediatric Blood and Marrow Transplant, Minneapolis, MN 55455

[2]University of Minnesota, Department of Biochemistry, Molecular Biology and Biophysics, Minneapolis, MN 55455

[3]Department of Pathology and Cancer Center Research and Treatment Center, University of New Mexico Health Sciences Center, Albuquerque, NM, USA

Abstract

There is accumulating evidence that mesenchymal stem cells (MSC) have their origin as perivascular cells (PVC) in vivo, but precisely identifying them has been a challenge, as they have no single definitive marker and are rare. We have developed a fluorescent transgenic vertebrate model in which PVC can be visualized in vivo based upon *sdf1* expression in the zebrafish. Prospective isolation and culture of s*df1*^{DsRed} PVC demonstrated properties consistent with MSC including prototypical cell surface marker expression; mesodermal differentiation into adipogenic, osteogenic and chondrogenic lineages; and the ability to support hematopoietic cells. Global proteomic studies performed by 2-dimensional liquid chromatography and tandem mass spectrometry revealed a high degree of similarity to human MSC and discovery of novel markers (CD99, CD151 and MYOF) that were previously unknown to be expressed by hMSC. Dynamic in vivo imaging during fin regeneration showed that PVC may arise from undifferentiated mesenchyme providing evidence of a PVC – MSC relationship. This is the first model, established

Corresponding Author. Troy Lund MSMS PhD MD FAAP, Assistant Professor, University of Minnesota, Pediatric Blood and Marrow Transplant Program, Stem Cell Institute, Global Pediatrics, MMC 366, 420 Delaware St SE, Minneapolis, MN 55455, (612) 625 4185, lundx072@umn.edu.
*equal contributors

Author Contribution Summary

TCL financial support, conception and design, collection and/or assembly of data, data analysis and interpretation, manuscript writing, final approval of manuscript
XP collection and/or assembly of data
ACK collection and/or assembly of data
PS collection and/or assembly of data
LH collection and/or assembly of data, data analysis and interpretation
TWM collection and/or assembly of data, data analysis and interpretation
MWS collection and/or assembly of data, data analysis and interpretation
DSL collection and/or assembly of data, data analysis and interpretation
JT manuscript writing, final approval of manuscript
BRB data, data analysis and interpretation, manuscript writing, final approval of manuscript

Conflict of Interest

Each author declares no conflict of interest.

in zebrafish, in which MSC can be visualized in vivo and will allow us to better understand their function in a native environment.

Introduction

Mesenchymal stem cells (MSC) are a component of the bone marrow niche and are thought to provide support to hematopoietic cells. Biologic characterization chiefly has been performed only after MSC have been culture expanded from the microenvironment in which they reside. MSC do not originate exclusively from the bone marrow, previous evidence shows that MSC also can be derived from multiple tissue sources[1, 2], suggesting that the ancestral cell of the MSC is common to most if not all tissues. Two previous reports suggested that a cell found on the abluminal surface of blood vessel, a perivascular cell (PVC), is a potential source for MSC[3, 4].

Early evidence for a PVC origin for MSC was provided by Crisan who identified PVC expression of CD146 (melanoma associated adhesion molecule), NG2 (glia cell marker), and platelet-derived growth factor receptor expression-β (PDGF-Rβ) expression. Flow cytometry sorted CD146 positive cells and cultured outgrowths on plastic dishes ultimately give rise to MSC, defined by CD73, CD90, and CD105 expression (and lacking mature hematologic or endothelial marker expression) and their ability to become adipogenic, osteogenic, or chondrogenic cells using in vitro differentiation assays[4]. Zannettino et al. showed that the vasculature of adipose tissue harbors CD146 and 3G5 (beta amyloid) co-expressing PVC which met the definition of MSCs based upon phenotype and in vitro differentiation capacity[5].

SDF1 was originally isolated from cultured bone marrow stromal cells that were consistent with MSC[6]. Recently, Ding et al showed that endothelial and perivascular cells express SDF1 in vivo using a transgenic *Sdf1* reporter mouse model[7]. Sugiyama reported that *Sdf1* expressing cells are located near sinusoidal endothelial cells or in the endosteal marrow region in a different *Sdf1* reporter mouse[8]. However, direct visualization of MSC ancestors as PVC and their isolation has been technically difficult[4].

In our previous work, we described the development an *sdf1a:DsRed* transgenic zebrafish which was the first animal model that allowed direct visualization of cells that produce high levels of stromal cell-derived factor-1 (Sdf1a) marked by fluorescent reporter expression. Given that Sdf1a is used by a number of developing organ systems for cell migration during development[9–12], we were not surprised to find that our *sdf1a:DsRed* transgenic zebrafish indicated *sdf1a* was expressed in multiple organs and cell types including gills, brain, and PVC[13].

Building on these prior observations, we have now prospectively isolated *sdf1*^{DsRed} PVC and have shown they express genes consistent with PVC. We have established a culture system for zebrafish PVC expansion in vitro and have shown that PVC can be tri-differentiated into mesodermal lineages and support the growth of hematopoietic cells in vitro. Tandem mass spectrometry analysis of cultured *sdf1*^{DsRed} PVC reveled their proteome to be similar to the human MSC proteome including cell surface proteins characteristic of

MSCs. Finally, during fin regeneration after amputation, *sdf1*^{DsRed} cells contributed to the mesenchyme of the newly developing bony rays prior to re-occupying the "perivascular niche". The *sdf1:DsRed* transgenic zebrafish will be a powerful tool to investigate the nature of PVCs and the PVC-MSC connection in further studies.

Materials and Methods

Zebrafish Strains and Fish husbandry

Fish were maintained by the University of Minnesota Zebrafish Core Facility according to standardized procedures[14] and with the approval of the International Animal Care and Use Committee, IACUC. Wild-type fish were obtained from Segrest Farms (Gibsonton, Florida) and bred in-house. The original *sdf1a:DsRed* transgenic was crossed with the *fli1:EGFP* as previously reported[15].

Microscopy

Live embryos, juvenile adult fish, and fish during fin regeneration experiments were anesthetized in 100 mg/L tricaine-S solution until no longer responsive when disturbed but still respiring. Fish were imaged using a QImaging Retiga 2000R camera and QCapture™ software on an inverted Leica DMI6000B microscope with a variety of objectives. Scale bars were placed via software integration. For z-stack imaging, confocal laser scanning microscopy was performed using a Zeiss LSM 510 inverted microscope system with a 20× air objective and appropriate filter sets. For z-stack imaging, confocal laser scanning microscopy was performed using a Zeiss LSM 510 inverted microscope system with a 20× air objective. Fish were anesthetized as above and placed in two- or four-well coverslip imaging chambers (Nunc). Excitation and emission filters were as follows: GFP, 488 nm excitation, emission BP 500–530 nm filter; RFP, 543 nm excitation, emission BP 565–615 nm filter.

Tail Digestion

Half of the caudal fin was removed using a sterile razor blade. Each fin was immersed for 10 seconds in 100% ethanol and placed separately in a 24 well plate in 100 μL PBS on ice while other fins were collected. The PBS was removed and replaced with 1:10,000 solution of bleach in PBS for 10 minutes at 25°C. Following bleaching, the fins were washed with 100 μL PBS three times for five minutes. Liberase was added to 0.01M HEPES in DMEM to create the digest media according to the manufacture's instructions, and 1mL of the digest media was added to each fin sample. Each sample was then mechanically shredded into smaller pieces using sterile scissors and incubated at 32°C for 30 minutes. Following incubation, the samples were dissociated manually using a pipette and placed on a shaker at 4°C overnight. The samples were dissociated again the next day with a pipette and passed through a 40-micron filter prior to downstream analyses.

Cell Culture

sdf1^{DsRed} PVC were isolated by flow cytometry gating on a DsRed positive cell population and maintained zebrafish cell culture media (250 mL L-15, 175 mL DMEM, 75 mL Ham's 12, 75mg sodium bicarbonate, 0.15M HEPES, 50 units penicillin/50 micrograms

streptomycin, 2 mM l-glutamine, 50 mL fetal bovine serum (FBS), 5 ng/ml selenium, 5 ng/ml human bFGF). Stromal cells appeared in about 2 – 3 weeks. The resulting cellular outgrowths were maintained and split at 80 – 90% confluence once or twice per week. Incubator conditions were 4% CO_2 and 5% O_2 and a temperature of 28°C. Human MSC were thawed from frozen stock and cultured as previously described[16].

Differentiations/Staining

See Supplemental Methods.

In Situ Hybridization

Fins were amputated in sterile, RNase free conditions, embedded in OCT, and flash frozen in dry-ice cooled isopentane. Frozen blocks were either stored at −80°C or immediately sectioned. Sections were taken at 8μm, allowed to dry for 10 minutes, and then fixed in 4% paraformaldehyde in PBS for 1 hour at room temperature (RT). *sdf1a* in situ hybridization and immunological detection was performed as previously described with the following deviations: slides were not covered with a coverslip during the overnight RNA probe hybridization, and slides were incubated at 37°C during the hybridization step[17].

Hematopoietic Co-culture

The *sdf1*^{DsRed} cells were grown to confluency in 24-well plate. 50,000 freshly isolated whole kidney marrow (WKM) cells from *bactin2:GFP* transgenic fish were place onto of the monolayer in zebrafish cell culture media for 16 days. Plastic only control wells contained no monolayer. After 16 days, cells were pipet aspirated and enumerated by counting on a flow cytometer using counting beads. For short-term transplant experiments, all the hematopoietic cells content of a single well (24-well) were transplanted into a recipient zebrafish that had received 20 Gy irradiation 48 hours prior. Seven days after transplant, recipient WKM was harvested and donor cell engraftment was determined by flow cytometry for GFP positive cells. In one experiment, 50,000 freshly isolated WKM cells were used in comparison.

Flow Cytometry

Cells were harvested using trypsin and stained with anti-myoferlin 7D2 (Abcam, ab76746), anti-CD151 conjugated to Allophycocyanin (Biolegend, #350405), or anti-CD99 conjugated to phycoerythrin (Biolegend, #318008) according to the manufacture's recommendations. Secondary antibodies were used when appropriate (Biolegend, #Poly4053). Cells were stained for 40 minutes at 4 C followed by once the addition of 3 milliliters of PBS, centrifugation at 1000 × g for five minutes and suspension in PBS prior to flow cytometry on a BD FACS Canto Flow Cytometer. Data analysis was performed using FlowJo (Tree Star, Inc, Ashland, OR)

RT-PCR

RNA was prepared using Trizol per the manufacture's protocol. RT-PCR was performed according to standard methods. Primers used in this study are listed in Supplemental Table 1. Often SYBR®Green (Invitrogen) quantitation was used, but occasionally TaqMan®

(ABI) primers were employed, in which case the product number is listed. The melting temperature was 60 C.

Endothelial Co-culture

Co-culture experiments were conducted using human umbilical vein endothelial cells (HUVECs, Lonza C2517A) and previously isolated and culture expanded *sdf1*^{DsRed} cells from the caudal fin of adult transgenic zebrafish. HUVECs were grown and maintained as instructed by the supplier. Each cell population was grown to approximately eighty percent confluency in their appropriate medium and fluorescently labeled as adherent cells to the flask using CellTracker™ Dyes (Invitrogen) according the manufacture's instructions. HUVECs were labeled using CellTracker™ Orange (Invitrogen C34551) and cultured *sdf1*^{DsRed} cells were labeled using CellTracker™ Green (Invitrogen C2925) at a final concentration of 1μM. Following labeling, 15,000 HUVECs and 10,000 culture expanded *sdf1*^{DsRed} cells were mixed together and grown on 100 μL of Matrigel™ (BD Biosciences) in a 96-well plate with EGM-2 media (Lonza). The cells were imaged 10–16 hours following plating, and the qualitative observations of HUVEC and perivascular cell branching were observed using a fluorescent microscopy as above.

Cross Section Immunohistochemistry

Fish fins were frozen in Tissue-Tek O.C.T compound (Sakura Finetek USA, Torrance, CA) and sectioned at 6 microns on a cryostat. Sections were fixed with a mixture of 3.7% paraformaldehyde, 10% Sucrose for 5 minutes at room temperature. Fins were rehydrated with PBS and blocked with 10% normal donkey serum for 1 hour (Jackson Immunoresearch, West Grove, PA). Primary antibody to DsRed (1:300) (Clontech, Mountain View, CA) was added for 1 hour, washed off with PBS, then mixed with primary antibody to GFP conjugated to FITC (1:200) (Rockland, Gilbertsville, PA) followed by a second secondary antibody which was donkey anti-rabbit-Cy3 (1:500), (Jackson Immunoresearch, West Grove, PA) was applied for 1 hour. Fins were washed with PBS and cover-slipped with hard set DAPI, 4,6-diamidino-2-phenylindole (Vector Labs, Burlingame, CA). Slides were imaged by confocal fluorescence microscopy (Olympus BX61, FV500, Olympus Optical, Tokyo, Japan).

Mass Spectrometry

See Supplemental Methods.

Fin Regeneration

Zebrafish were anesthetized in 100 mg/L tricaine-S solution until it was no longer responsive when disturbed. While anesthetized, the caudal fin was amputated using a sterile razor blade. Photos of the regenerating fin were captured every 24 hours. All photos were taken using an inverted fluorescent microscope as described above. Unless otherwise stated, regeneration images were taken using a 10× objective lens. Fluorescent images were pseudo-colored in Adobe Photoshop CS4 according to the emission of the fluorophore, and multiple color channels within a single field of view were merged together.

Results

Although *sdf1*^{DsRed} PVC were found in multiple organs as we have previously described[13], we focused on caudal tail isolation, a site of high prominence and visualization (Figure 1, Supplemental Figures 1 and 2). The *sdf1*^{DsRed} PVC were most evident when we crossed our *sdf1a:DsRed* transgenic to the *fli1:EGFP* transgenic zebrafish which robustly illustrates the vasculature composed of EGFP positive endothelial cells[18]. High magnification revealed *sdf1*^{DsRed} cells notably located on the abluminal surface of various blood vessels including both the central vessels of the bony rays as well as bridging vessels between rays as shown in Figure 1(B–D). This is the first time perivascular cells have been seen using in vivo live fluorescent microscopy in a transgenic animal.

The progenitors to the *sdf1*^{DsRed} PVC start to become visible as early as 3 days post fertilization (dpf) as part of the developing tail fin, but are more clearly evident at 8 dpf (Supplemental Figure 3). The cells appear to originate in the undefined mesoderm of the developing tail fin posterior to the developing spinal cord (which also shows distinct DsRed positivity). As the larval zebrafish continue to undergo tail fin development and the vasculature grows caudally during the juvenile stage of development, distinct PVC can be visualized abluminal to vascular endothelial cells at 21 dpf (Supplemental Figure 3).

MSC from human and murine sources have been proposed to originate from PVC in vivo[3, 4]. Therefore, our primary interest was to determine if *sdf1*^{DsRed} PVC could be a source for MSC in the zebrafish. Using flow cytometry sorting, we were able to isolate *sdf1*^{DsRed} cells from the tail fin after enzymatic digestion of the tissue and 8 – 10 % (n = 20 animals) of the cells were DsRed positive (Figure 2). To determine if *sdf1*^{DsRed} PVC expressed putative markers of PVC other than *sdf1*, RNA was extracted from flow cytometry-sorted cells obtained from *sdf1a:DsRed-fli1:EGFP* double transgenic animals followed by quantitative RT-PCR for genes of interest. The previously reported PVC associated genes smooth muscle actin (*acta2*), chondroitin sulfate proteoglycan *(cspg)*, transgelin (*tgln*), and cadherin5 (*cdh5*) were all significantly upregulated in *sdf1*^{DsRed} positive cells as compared to *fli1*^{EGFP} endothelial cells, and the *fli1* gene showed increased expression in the EGFP^{+} endothelial cells as expected while *cd45* was absent in both cell types (figure 2B). Although there is no single specific marker for either PVC or MSC, expression of these markers have been consistently reported to be expressed by both by PVC and MSC in various studies[19–21].

A criterion for MSC is plastic adherence after isolation from the tissue source being tested (whether bone marrow, fat, or umbilical cord blood in origin), and subsequent tissue culture outgrowth[22]. We and others have previously developed successful culture systems for zebrafish stromal cells derived from organ outgrowths[23],[24]. We prospectively sorted *sdf1*^{DsRed} PVC by flow cytometry based on DsRed expression followed by plating onto tissue culture treated plastic dishes. After 24 hours of culture, *sdf1*^{DsRed} PVC adhered to the bottom of the culture plate acquiring a flattened appearance, and were of irregular sizes and fibroblastoid in shape. After about one week in culture, phase contrast microscopy visualization revealed that cultured cells continued to have a shape similar to that of MSC - being somewhat flattened and fibroblastoid (Figure 2C). Several (n = 5) independent stromal lines were established. Cultured *sdf1*^{DsRed} PVC were evaluated for prototypical markers of

MSC including ecto-5'-nucleotidase (*nt5e*), *thy-1, and* endoglin–like *(engl)* gene expression (the human homologs being CD73, CD90, and CD105) and found to be expressed (Figure 2D). RT-PCR of sorted *sdf1*^{DsRed} PVC also showed the presence of *nt5e*, *thy-1*, and *engl* mRNA indicating their expression prior to in vitro culture expansion (Supplemental Figure 4). Cultured *sdf1*^{DsRed} PVC did not express hematopoietic markers including *cd45*, *gata1*, *lck* and *mpx*.

MSC express receptors for fibroblast growth factor (FGFRs) and are growth responsive to FGF[25]. Our expansion culture medium contained 5 ng/mL human recombinant basic FGF. Therefore, we next determined whether culture expanded *sdf1*^{DsRed} PVC were growth responsive to FGF. Similar to what has been reported for MSC, Figure 2E shows the culture-expanded *sdf1*^{DsRed} PVC expressed *fgfr1a and fgfr2* and displayed a dose-responsive increase in growth with basic FGF supplementation. Unlike human MSC, which have a limited number of population doublings, the zebrafish culture-expanded *sdf1*^{DsRed} PVC do not undergo senescence with PVCs being in continuous culture for more than 18 months (> 100 population doublings) with no decrease in growth potential (data not shown).

After determining that culture-expanded *sdf1*^{DsRed} PVC adhere to plastic and express genes similar to MSC, we next performed differentiation of the cells into the classic mesodermal-derived osteogenic, adipogenic, and chondrogenic lineages. As shown in Figure 3A, after 3 to 4 weeks of differentiation in adipogenesis promoting medium, the adipogenic genes of fatty acid binding protein 4 *(fabp4)* and *leptina* were highly increased in expression. Additionally, expression of crystalline, beta A1a *(cryba1a)*, was absent in undifferentiated cells, but present after adipogenic differentiation. Furthermore, adipogenic differentiated cells showed classic lipid vacuolization and stained positive with Oil-Red-O. Culture expanded *sdf1*^{DsRed} PVC placed into chondrogenic conditions for 4 weeks showed increased expression of the chondrocyte-associated genes *sox9a*, *col10a1*, and cartilage oligomeric matrix protein *(comp)* and toluidine blue staining showed glycosaminoglycans were increased (Figure 3B). Differentiation in osteogenic conditions induced the expression of *runx2*, *osteocalcin*, and alkaline phosphatase (*alp*) as determined by qRT-PCR, but Alizarin red staining did not reveal the bright red confluent layer of calcium laden osteocytes which we commonly observe with our human MSC differentiations (Figure 3C)[16]. Instead, we found scattered pink-staining collections of cell clusters akin to bony osteophytes that were absent in undifferentiated cell cultures, which suggests a partial differentiation process.

These data suggest that culture-expanded *sdf1*^{DsRed} PVC from the zebrafish can give rise to cells with an MSC phenotype in the proper culture conditions. The osteogenic differentiation appears to be incomplete which could be due to a weaker propensity for osteogenic differentiation or possibly due to improper media formulation and lack of zebrafish specific factors driving osteogenic differentiation. Another likely possibility is that even though culture expanded *sdf1*^{DsRed} PVC appear homogenous during in vitro culture, populations with mixed lineages perhaps with different differentiation potentials are likely present.

Human MSC have the ability to support the expansion of hematopoietic stem and progenitor cells in vitro[26]. We have previously shown that zebrafish stromal cells have a similar ability[24]. We next explored the capacity of the culture-expanded *sdf1*^{DsRed} PVC to support

hematopoietic cells. Our initial RT-PCR screen for genes expressed by culture-expanded *sdf1*^{DsRed} PVC showed the expression of several genes important in the growth and maintenance of hematopoietic cells including: several *notch* family members as well as *bmp1*, and *flt1* (Figure 4A). We next performed co-culture experiments with 50,000 hematopoietic cells from *bactin2:GFP* transgenic zebrafish seeded onto a monolayer of culture-expanded *sdf1*^{DsRed} PVC versus hematopoietic cells on plastic alone for 16 days. We found that culture-expanded *sdf1*^{DsRed} PVC gave a significant survival advantage (2 – 3.5 fold, $p < 0.001$) to the hematopoietic cells when compared to plastic alone (Figure 4B), though significant hematopoietic cell expansion was not noted. The survival advantage may be through engagement of cell maintenance pathways or because of decreased programmed cells death. The lack of true expansion is most likely due to the absence of supplemental hematopoietic growth factors which are not commonly available.

To evaluate short-term engraftment potential, 50,000 hematopoietic cells from *bactin2:GFP* transgenic zebrafish co-cultured with PVC as before were transplanted into zebrafish that previously received sublethal irradiation (2 days prior), and donor engraftment was assessed 7 days later by flow cytometry (Figure 4C). There was no difference between co-cultured marrow cells and freshly isolated marrow cells in terms of their ability to home and provide short term ($p = 0.65$). We next compared the short-term engraftment of hematopoietic cells co-cultured on *sdf1*^{DsRed} PVC versus plastic (as in Figure 4B). After 16 days in culture, the entire content of a well was injected into zebrafish that previously received sublethal irradiation (2 days prior). A significant short-term engraftment advantage ($p < 0.001$) when measured 7 days after transplant was found for hematopoietic cells in PVC co-culture experiments versus on plastic alone (Figure 4D). These data show that hematopoietic cells when co-cultured with *sdf1*^{DsRed} PVC cells maintain survival, and conserve their native homing and at least short-term engraftment abilities.

To understand the biology of culture-expanded *sdf1*^{DsRed} PVC and how they may be related to human MSC, we performed a global proteomic profile analysis using 2-dimensional liquid chromatography and tandem mass spectrometry. We isolated human MSC from three independent donor bone marrow samples for comparative analysis to three independently isolated zebrafish culture-expanded *sdf1*^{DsRed} PVC (lines H, X, and Y). Whole cell lysates were prepared from confluent T-150 culture flasks, and subject to reversed phase (C18 resin) chromatography at pH 10 (first dimension) with fraction collection followed by reversed phase (C18 resin) chromatography at pH 3 (the second dimension) online with mass spectrometry. MS analysis was performed on an Orbitrap™ mass spectrometer. The resulting protein identifications were derived from those proteins with a 2-peptide minimum identification, a confidence interval (CI) of 95% at the peptide level and a CI of 90% at the protein level (see Supplemental Methods for data analysis). Protein lists were combined and redundant hits eliminated. We collectively identified 2141 proteins in zebrafish culture-expanded *sdf1*^{DsRed} PVC (from 15697 unique peptides) and 2337 proteins in hMSC (from 22040 unique peptides). The average molecular weight was similar in both proteomes at 64.0 kDa for zebrafish and 69.2 kDa for hMSC with similar ranges (Figure 5). Next, proteins were cross-referenced by Uniprot accession numbers and Ingenuity Pathway Analysis (IPA®) was performed. The percentage of proteins by subcellular location was

remarkably similar between the two species with the majority of the proteins identified being of cytoplasmic origin, followed by nuclear proteins, then unknown or plasma membrane proteins, and lastly extracellular proteins. Further analysis of protein relationships based on gene ontology (using GO terms) revealed that many of the zebrafish proteins were involved with tissue development (specifically connective tissue) and skeletal/muscular system development. Similarly, hMSC proteins ranked highest in tissue development (again specifically connective tissue). We next derived gene names from the Uniprot identifications generating subsets of 1694 proteins in the zebrafish, and 2305 proteins in hMSC. We next derived gene names from the Uniprot identifications; final subsets contained 1694 zebrafish proteins and 2305 hMSC proteins. The union of the two data sets showed 1102 common proteins consisting of 65% of the zebrafish culture-expanded *sdf1*^{DsRed} PVC proteome, and 48% of the hMSC proteome. The subcellular location and gene ontogeny of the common proteins was similar to the original groups. We were curious if uncharacterized hMSC proteins could be discovered using this data, and upon evaluating the union of the two proteomes, we chose three novel cell surface proteins common to both zebrafish and hMSC protein subsets which have not been previously shown to be expressed on hMSC to verify their expression: CD99 (a Ewing's sarcoma marker), CD151, and myoferlin (a potential modifier of muscular dystrophy). These proteins have been little studied in terms of any relationship to MSC, though we showed confirmation of their expression on hMSC using flow cytometry staining (Figure 5E). These data show that hMSC and zebrafish cultured *sdf1*^{DsRed} PVC have a high degree of proteomic similarity and new MSC proteins can be discovered by the interrogation of zebrafish *sdf1*^{DsRed} cells. Furthermore, cultured *sdf1*^{DsRed} PVC may represent a novel zebrafish source of MSC.

To determine whether or not culture expanded *sdf1*^{DsRed} PVC could be co-cultured with human endothelial cells to evaluate for morphological changes, we utilized human umbilical vein endothelial cells (HUVECs) in co-culture experiments. Culture-expanded *sdf1*^{DsRed} PVC showed no cellular organization when cultured on a matrigel substrate alone either in their native media or endothelial growth media (Figure 6A). After the perivascular cells were placed into culture together with HUVECs, the zebrafish culture expanded *sdf1*^{DsRed} PVC became substantially more networked and co-aligned (becoming peri-endothelial) with the HUVECs (Figure 6B). This experiment shows that endothelial cells can influence the behavior of culture expanded *sdf1*^{DsRed} PVC.

The prior experiments described many of the in vitro properties of culture-expanded *sdf1*^{DsRed} PVC and their similarity to hMSC. MSC have been used to facilitate the repair of bone and cartilage injuries, but whether this occurs in the de novo setting is unknown[27–29]. We chose to utilize a model of tail fin regeneration to evaluate the behavior of *sdf1*^{DsRed} PVC in this process. After tail amputation in *sdf1a:DsRed* × *fli1:EGFP* transgenic animals, there was *sdf1:DsRed* expression at the healing edge 1 day post amputation (dpa) as previously described[30]. While rapid vascular regeneration occurred within in 72 hours post amputation, robust DsRed expression with cellular organization became very strong at 4 – 5 dpa (Figure 7) when the *sdf1*^{DsRed} cells appeared to organize into segments of the regenerating bony ray. Interestingly, it was not until 6–7 dpa when the reappearance of *sdf1*^{DsRed} cells in a perivascular location was observed around the neovasculature

(Supplemental Figure 5). The new PVCs seemed to be derived from the surrounding mesenchyme (versus having migrated from a distal source), which suggests that the newly formed mesenchyme was a source for *sdf1*^{DsRed} perivascular cells. This model demonstrates the in vivo contribution of *sdf1* expressing cells to the regenerating fin structure as well as the derivation of PVC during vasculature regeneration and will be useful in future studies to determine in vivo PVC function, which until now has been difficult in mammalian systems.

Discussion

The zebrafish is an excellent model to visually observe cellular anatomy given its optical translucence as an embryo as well the recent development of “transparent” adult animals harboring a pigmentation defect[31]. The creation of the *sdf1a:DsRed* reporter allowed us to visualize DsRed positive, Sdf1a-producing cells. It is well known that *SDF1* is expressed by a wide variety of cell types, although its original discovery and purification was from bone marrow stromal cells that were not termed MSC at the time of discovery, the stromal cells most likely fulfilled criteria for MSC[32].

Our *sdf1a:DsRed* transgenic allows for the observation of distinct PVC in their native environment. We were able to isolate and culture-expand zebrafish *sdf1*^{DsRed} PVC and showed they fulfilled criteria for classification as MSC (zMSC). One clear difference between zMSC and hMSC is the growth potential of the cells. Human MSC are limited in the number of cell divisions they can undergo with a limit of around 50 population doublings[33–35]. Whereas in zMSC (and other zebrafish stromal cell lines) there is no declination in doubling time nor change in cellular morphology even after 1–2 years in culture reflecting over 100 population doubling times[23, 24]. This phenomenon is most likely related to the constitutive activation of the telomerase gene that we and others have described in zebrafish cells[36–38]. Zebrafish have the ability to regenerate several organ systems repetitively. Even after multiple rounds of tail regeneration, the telomeres seem to maintain their full length and telomerase function is intact[36]. Maintaining “mesenchymal” cells with unlimited cell division potential would certainly contribute to the ability to continually regenerate tissues after damage.

Our data from the proteomic interrogation of both zebrafish and human MSC revealed significant overlap in protein expression. The subcellular distribution was not surprising and corresponded to the native distribution of most proteins (cytoplasmic abundance followed by nuclear and extracellular/membrane localization respectively). The most interesting finding of this analysis was the identification of new cell surface proteins. Expression of CD99 and myoferlin have not been shown to be present on MSC, while CD151 was detected in a prior proteomic interrogation of hMSC microvesicles and may contribute to microvesicle fusion, although other studies showed it was important in angiogenesis[39, 40]. CD99 is a known marker of neuroectodermal cancers including Ewing’s sarcoma but is also expressed in wide variety of other cell types including lymphocytes diminishing its novelty, though its function on MSC is unknown[41, 42]. Myoferlin (MYOF) is an ancient protein involved in internal membrane bound organelle’s ability to fuse with the plasma membrane, and defects in the Ferlin family cause a form of muscular dystrophy due to poor sarcolemma repair[43]. Recent studies have focused on MYOF expression in breast cancer and the regulation of the

mesenchymal to epithelial state where expression of MYOF favors a more invasive mesenchymal state[44]. To our knowledge, expression of MYOF has not been shown on MSC. Future exploration of these and other proteins we have determined will be help to broaden our understanding of MSC biology, both in vivo and in vitro.

MSC have had a wide variety of functions ascribed to them including wound healing, vascular healing, and organ damage repair[29, 45, 46]. We visualized the contribution of *sdf1*^{DsRed} cells to fin regeneration, a model for limb regeneration. It has been specifically shown that assessing gene expression by standard whole-mount in situ hybridization techniques in the regenerating fin is limited due to poor probe penetration through the "mesenchymal" tissue of the fin as it undergoes repair[47]. The advantage to using transgenic reporters like *sdf1a:DsRed* in our experiments is that visualization of the cellular events is easily accomplished in live animals. One disadvantage to using DsRed is its slow maturation time to form tetramers (24h hours) and its long half-life (4.5 days) which may make it difficult to determine rapid changes in gene expression[48], though the extended DsRed half-life does make it useful to track cellular movement over long periods of time.

The intra-ray tissue of the caudal fin is composed of vessels, nerves, osteoblasts, pigment cells, and "fibroblast-like" cells[49]. The regenerating blastema has been proposed to be derived from intra-ray "mesenchymal" cells or "fibroblast-like" cells[50, 51]. Work by Knopf et al. has demonstrated that the regenerating fin blastema is also partly composed of dedifferentiated osteoblasts. We propose that these fibroblast-like cells are *sdf1*^{DsRed} mesenchymal cells illustrated in our model of regeneration, though the origin of the regenerating *sdf1*^{DsRed} mesenchymal cells is still unknown. Possibilities include migration from the injured fin ray stump, dedifferentiation from proximal fin-ray-osteoblasts, or dedifferentiation from proximal fin-ray-epidermal cells. Crossing our transgenic with other reporter lines (osteoblast and epidermal cell reporters) will help answer the question of where the blastemal mesenchymal cells originate.

Our observation of *sdf1*^{DsRed} cells developing within 1 – 2 dpa in the blastema is consistent with prior reported *sdf1* expression in regenerating fins[30, 52]. The blastema *sdf1* expression reported by Dufourcq was downregulated at 5 dpa, while our observations suggest that *sdf1*^{DsRed} cells are quite evident early after amputation, increasing over the 5 dpa course. The prior experiments used in situ hybridization to determine *sdf1* expression and given that probe penetration becomes very limited during fin regeneration, we believe *sdf1* expression may have been underestimated. Additionally, the long half-life of DsRed allows us to track *sdf1* expressing cells over longer periods of time to get a better understanding of the structure changes occurring during regeneration.

Aside from understanding the contribution of *sdf1*^{DsRed} mesenchymal cells to the regenerating tail fin bony ray, our model system will useful for interrogating the function of PVC as they are very evident with in vivo imaging. Surprisingly, the PVC in the regenerating fin did not reappear until multiple days after amputation and neovascularization (6 – 7 dpa shown in Supplemental Figure 3). This suggests that PVCs are not required during the immediate development of the newly forming vessels. Our observation that the mesenchymal cells arise before the appearance of PVC suggests that the *sdf1*^{DsRed} PVC

either migrate or differentiate from mesenchymal tissue to adopt an abluminal location on the vessel. Whether the new *sdf1*^{DsRed} PVC have adopted additional functional properties that are distinct from the *sdf1*^{DsRed} mesenchymal cells remains unexplored.

We did observe qualitatively that the vasculature prior to PVC presence had a larger diameter, more tortuous appearing, and have increased numbers of branch points as compared to vasculature after PVC appeared. In in vitro endothelial tube assembly models, Stratman et al recently showed that PVC are recruited to endothelial tubes and contribute to basement membrane deposition and endothelial "stabilization" that result in smaller diameter tubes[53, 54]. A second study has shown that PVC can also play a role in "selective pruning" during vasculature development in vitro and in vivo via endosialin (CD248) expression on PVC[55].

Finally, detailed experiments by Bell et al indicate that a critical function of murine brain pericytes is to stabilize the blood-brain-barrier (BBB), and pericyte loss leads to increased BBB permeability with subsequent brain accumulation of protein and other macromolecules[56, 57]. Murine pericytes interact both with astrocytes and endothelial cells via complex signaling networks to maintain vascular integrity with participation of *ApoE*, Low-density lipoprotein receptor-related protein 1 (*Lrp1*), and Cyclophilin A (*CypA*) as important factors. The pericytes identified by Bell et al are analogous in their abluminal anatomical location to the perivascular cells identified in our work, and we observed some *sdf1*^{DsRed} perivascular cells in the brains of our zebrafish though the former work utilized *Pdgfrβ* expression to identify pericytes in contrast to our *sdf1a* promoter transgenic expression. Our own preliminary (and non-quantified) dye-exclusion studies during tail fin regeneration indicted that vascular integrity was restored within a similar to time frame to perivascular re-appearance at about 6 – 7 dpa (data not shown). Whether our *sdf1*^{DsRed} cells are exactly equivalent to PDGFRβ-expressing pericytes cells is unknown, but the advantages conferred by a zebrafish system will allow further experiments that can broaden the understanding of the complex PVC-endothelium relationship through live imaging studies.

Conclusion

In conclusion, we have developed a model in which PVC can be visualized in an in vivo setting based on *sdf1* expression. Prospective isolation and culture of the *sdf1*^{DsRed} PVC allowed us to demonstrate properties consistent with that of MSC including cell surface marker expression, FGF responsiveness, mesodermal differentiation, and hematopoietic cell support. Proteomic studies revealed a high degree of similarity to hMSC and the description of novel MSC markers (CD99, CD151 and MYOF). Dynamic in vivo imaging of the *sdf1*^{DsRed} expressing cells show that PVC may arise from undifferentiated mesenchyme, which provides further evidence of the PVC – MSC connection. This model system will allow us to better understand their contribution to vasculature and tissue regeneration processes.

Supplementary Material

Refer to Web version on PubMed Central for supplementary material.

Acknowledgments

Research reported in this publication was supported by the National Heart, Lung and Blood Institute of the National Institutes of Health under award number K08HL108998, an American Society for Blood and Marrow Transplantation Young Investigator Award, and an American Society for Hematology Scholar Award (TCL). DSL was supported by the New Mexico Spatiotemporal Modeling Center NIH P50GM085273. The content is solely the responsibility of the authors and does not necessarily represent the official views of the National Institutes of Health. We would like to acknowledge the use of the Olympus and Zeiss confocal microscopes made available through a National Center for Research Resources Shared Instrumentation Grant (#1 S10 RR16851 and #1 S10 RR16851 respectively).

References

1. Prunet-Marcassus B, Cousin B, Caton D, et al. From heterogeneity to plasticity in adipose tissues: site-specific differences. Exp Cell Res. 2006; 312:727–736. [PubMed: 16386732]
2. da Silva Meirelles L, Caplan AI, Nardi NB. In search of the in vivo identity of mesenchymal stem cells. Stem Cells. 2008; 26:2287–2299. [PubMed: 18566331]
3. Corselli M, Chen CW, Crisan M, et al. Perivascular ancestors of adult multipotent stem cells. Arterioscler Thromb Vasc Biol. 2010; 30:1104–1109. [PubMed: 20453168]
4. Crisan M, Yap S, Casteilla L, et al. A perivascular origin for mesenchymal stem cells in multiple human organs. Cell Stem Cell. 2008; 3:301–313. [PubMed: 18786417]
5. Zannettino AC, Paton S, Arthur A, et al. Multipotential human adipose-derived stromal stem cells exhibit a perivascular phenotype in vitro and in vivo. J Cell Physiol. 2008; 214:413–421. [PubMed: 17654479]
6. Tashiro K, Tada H, Heilker R, et al. Signal sequence trap: a cloning strategy for secreted proteins and type I membrane proteins. Science. 1993; 261:600–603. [PubMed: 8342023]
7. Ding L, Morrison SJ. Haematopoietic stem cells and early lymphoid progenitors occupy distinct bone marrow niches. Nature. 2013; 495:231–235. [PubMed: 23434755]
8. Sugiyama T, Kohara H, Noda M, et al. Maintenance of the hematopoietic stem cell pool by CXCL12-CXCR4 chemokine signaling in bone marrow stromal cell niches. Immunity. 2006; 25:977–988. [PubMed: 17174120]
9. Chong SW, Nguyet LM, Jiang YJ, et al. The chemokine Sdf-1 and its receptor Cxcr4 are required for formation of muscle in zebrafish. BMC Dev Biol. 2007; 7:54. [PubMed: 17517144]
10. Chalasani SH, Sabelko KA, Sunshine MJ, et al. A chemokine, SDF-1, reduces the effectiveness of multiple axonal repellents and is required for normal axon pathfinding. J Neurosci. 2003; 23:1360–1371. [PubMed: 12598624]
11. Chalasani SH, Baribaud F, Coughlan CM, et al. The chemokine stromal cell-derived factor-1 promotes the survival of embryonic retinal ganglion cells. J Neurosci. 2003; 23:4601–4612. [PubMed: 12805300]
12. Doitsidou M, Reichman-Fried M, Stebler J, et al. Guidance of primordial germ cell migration by the chemokine SDF-1. Cell. 2002; 111:647–659. [PubMed: 12464177]
13. Lund TC, Glass TJ, Patrinostro X, et al. Stromal cell-derived factor-1 and hematopoietic cell homing in an adult zebrafish model of hematopoietic cell transplantation. Blood. 2011; 118:766–774. [PubMed: 21622651]
14. Westerfield, M. The zebrafish book : a guide for the laboratory use of zebrafish (Brachydanio rerio). Eugene, OR: M. Westerfield; 1993.
15. Lund TC, Glass TJ, Patrinostro X, et al. Stromal cell-derived factor-1 (SDF-1) and hematopoietic cell homing in an adult zebrafish model of hematopoietic cell transplant. Blood. 2011
16. Lund TC, Kobs A, Blazar BR, et al. Mesenchymal stromal cells from donors varying widely in age are of equal cellular fitness after in vitro expansion under hypoxic conditions. Cytotherapy. 2010; 12:971–981. [PubMed: 20807020]
17. Panoskaltsis-Mortari A, Bucy RP. In situ hybridization with digoxigenin-labeled RNA probes: facts and artifacts. BioTechniques. 1995; 18:300–307. [PubMed: 7727134]
18. Lawson ND, Weinstein BM. In Vivo Imaging of Embryonic Vascular Development Using Transgenic Zebrafish. Developmental Biology. 2002; 248:307–318. [PubMed: 12167406]

19. Wein F, Pietsch L, Saffrich R, et al. N-cadherin is expressed on human hematopoietic progenitor cells and mediates interaction with human mesenchymal stromal cells. Stem Cell Res. 2010; 4:129–139. [PubMed: 20116358]
20. Kozanoglu I, Boga C, Ozdogu H, et al. Human bone marrow mesenchymal cells express NG2: possible increase in discriminative ability of flow cytometry during mesenchymal stromal cell identification. Cytotherapy. 2009; 11:527–533. [PubMed: 19462316]
21. Salem HK, Thiemermann C. Mesenchymal stromal cells: current understanding and clinical status. Stem Cells. 2010; 28:585–596. [PubMed: 19967788]
22. Chamberlain G, Fox J, Ashton B, et al. Concise review: mesenchymal stem cells: their phenotype, differentiation capacity, immunological features, and potential for homing. Stem Cells. 2007; 25:2739–2749. [PubMed: 17656645]
23. Stachura DL, Reyes JR, Bartunek P, et al. Zebrafish kidney stromal cell lines support multilineage hematopoiesis. Blood. 2009; 114:279–289. [PubMed: 19433857]
24. Lund TC, Glass TJ, Somani A, et al. Zebrafish stromal cells have endothelial properties and support hematopoietic cells. Exp Hematol. 2012; 40:61–70. e61. [PubMed: 21920471]
25. Coutu DL, Francois M, Galipeau J. Inhibition of cellular senescence by developmentally regulated FGF receptors in mesenchymal stem cells. Blood. 2011; 117:6801–6812. [PubMed: 21527526]
26. Caplan AI, Dennis JE. Mesenchymal stem cells as trophic mediators. J Cell Biochem. 2006
27. Erickson IE, Kestle SR, Zellars KH, et al. Improved cartilage repair via in vitro pre-maturation of MSC-seeded hyaluronic acid hydrogels. Biomedical materials. 2012; 7:024110. [PubMed: 22455999]
28. Jones V. Meeting educational needs: postgraduate diploma/MSc in wound healing and tissue repair. Journal of wound care. 2001; 10:277–279. [PubMed: 12964348]
29. Bruder SP, Fink DJ, Caplan AI. Mesenchymal stem cells in bone development, bone repair, and skeletal regeneration therapy. J Cell Biochem. 1994; 56:283–294. [PubMed: 7876320]
30. Dufourcq P, Vriz S. The chemokine SDF-1 regulates blastema formation during zebrafish fin regeneration. Development Genes and Evolution. 2006; 216:635–639. [PubMed: 16586100]
31. White RM, Sessa A, Burke C, et al. Transparent adult zebrafish as a tool for in vivo transplantation analysis. Cell Stem Cell. 2008; 2:183–189. [PubMed: 18371439]
32. Shirozu M, Nakano T, Inazawa J, et al. Structure and chromosomal localization of the human stromal cell-derived factor 1 (SDF1) gene. Genomics. 1995; 28:495–500. [PubMed: 7490086]
33. Shay JW, Wright WE. Hayflick, his limit, and cellular ageing. Nature Reviews Molecular Cell Biology. 2000; 1:72–76.
34. Baxter MA, Wynn RF, Jowitt SN, et al. Study of telomere length reveals rapid aging of human marrow stromal cells following in vitro expansion. Stem Cells. 2004; 22:675–682. [PubMed: 15342932]
35. Banfi A, Muraglia A, Dozin B, et al. Proliferation kinetics and differentiation potential of ex vivo expanded human bone marrow stromal cells: Implications for their use in cell therapy. Exp Hematol. 2000; 28:707–715. [PubMed: 10880757]
36. Lund TC, Glass TJ, Tolar J, et al. Expression of telomerase and telomere length are unaffected by either age or limb regeneration in Danio rerio. PLoS One. 2009; 4:e7688. [PubMed: 19893630]
37. Kishi S, Uchiyama J, Baughman AM, et al. The zebrafish as a vertebrate model of functional aging and very gradual senescence. Exp Gerontol. 2003; 38:777–786. [PubMed: 12855287]
38. Elmore LW, Norris MW, Sircar S, et al. Upregulation of telomerase function during tissue regeneration. Experimental biology and medicine. 2008; 233:958–967. [PubMed: 18480423]
39. Kim HS, Choi DY, Yun SJ, et al. Proteomic analysis of microvesicles derived from human mesenchymal stem cells. Journal of proteome research. 2012; 11:839–849. [PubMed: 22148876]
40. Bailey RL, Herbert JM, Khan K, et al. The emerging role of tetraspanin microdomains on endothelial cells. Biochem Soc Trans. 2011; 39:1667–1673. [PubMed: 22103505]
41. Dworzak MN, Fritsch G, Buchinger P, et al. Flow cytometric assessment of human MIC2 expression in bone marrow, thymus, and peripheral blood. Blood. 1994; 83:415–425. [PubMed: 7506950]

42. Rocchi A, Manara MC, Sciandra M, et al. CD99 inhibits neural differentiation of human Ewing sarcoma cells and thereby contributes to oncogenesis. J Clin Invest. 2010; 120:668–680. [PubMed: 20197622]
43. Liu J, Aoki M, Illa I, et al. Dysferlin, a novel skeletal muscle gene, is mutated in Miyoshi myopathy and limb girdle muscular dystrophy. Nat Genet. 1998; 20:31–36. [PubMed: 9731526]
44. Li R, Ackerman WEt, Mihai C, et al. Myoferlin depletion in breast cancer cells promotes mesenchymal to epithelial shape change and stalls invasion. PLoS One. 2012; 7:e39766. [PubMed: 22761893]
45. Tran N, Li Y, Maskali F, et al. Short-term heart retention and distribution of intramyocardial delivered mesenchymal cells within necrotic or intact myocardium. Cell Transplant. 2006; 15:351–358. [PubMed: 16898229]
46. Madlambayan GJ, Butler JM, Hosaka K, et al. Bone marrow stem and progenitor cell contribution to neovasculogenesis is dependent on model system with SDF-1 as a permissive trigger. Blood. 2009; 114:4310–4319. [PubMed: 19717647]
47. Smith A, Zhang J, Guay D, et al. Gene expression analysis on sections of zebrafish regenerating fins reveals limitations in the whole-mount in situ hybridization method. Developmental dynamics : an official publication of the American Association of Anatomists. 2008; 237:417–425. [PubMed: 18163531]
48. Mirabella R, Franken C, van der Krogt GN, et al. Use of the fluorescent timer DsRED-E5 as reporter to monitor dynamics of gene activity in plants. Plant physiology. 2004; 135:1879–1887. [PubMed: 15326279]
49. Knopf F, Hammond C, Chekuru A, et al. Bone regenerates via dedifferentiation of osteoblasts in the zebrafish fin. Developmental cell. 2011; 20:713–724. [PubMed: 21571227]
50. Nechiporuk A, Keating MT. A proliferation gradient between proximal and msxb-expressing distal blastema directs zebrafish fin regeneration. Development. 2002; 129:2607–2617. [PubMed: 12015289]
51. Poss KD, Keating MT, Nechiporuk A. Tales of regeneration in zebrafish. Developmental dynamics : an official publication of the American Association of Anatomists. 2003; 226:202–210. [PubMed: 12557199]
52. Laudet V, Bouzaffour M, Dufourcq P, et al. Fgf and Sdf-1 Pathways Interact during Zebrafish Fin Regeneration. PLoS ONE. 2009; 4:e5824. [PubMed: 19503807]
53. Stratman AN, Malotte KM, Mahan RD, et al. Pericyte recruitment during vasculogenic tube assembly stimulates endothelial basement membrane matrix formation. Blood. 2009; 114:5091–5101. [PubMed: 19822899]
54. Stratman AN, Schwindt AE, Malotte KM, et al. Endothelial-derived PDGF-BB and HBEGF coordinately regulate pericyte recruitment during vasculogenic tube assembly and stabilization. Blood. 2010; 116:4720–4730. [PubMed: 20739660]
55. Simonavicius N, Ashenden M, van Weverwijk A, et al. Pericytes promote selective vessel regression to regulate vascular patterning. Blood. 2012; 120:1516–1527. [PubMed: 22740442]
56. Bell RD, Winkler EA, Sagare AP, et al. Pericytes control key neurovascular functions and neuronal phenotype in the adult brain and during brain aging. Neuron. 2010; 68:409–427. [PubMed: 21040844]
57. Bell RD, Winkler EA, Singh I, et al. Apolipoprotein E controls cerebrovascular integrity via cyclophilin A. Nature. 2012; 485:512–516. [PubMed: 22622580]

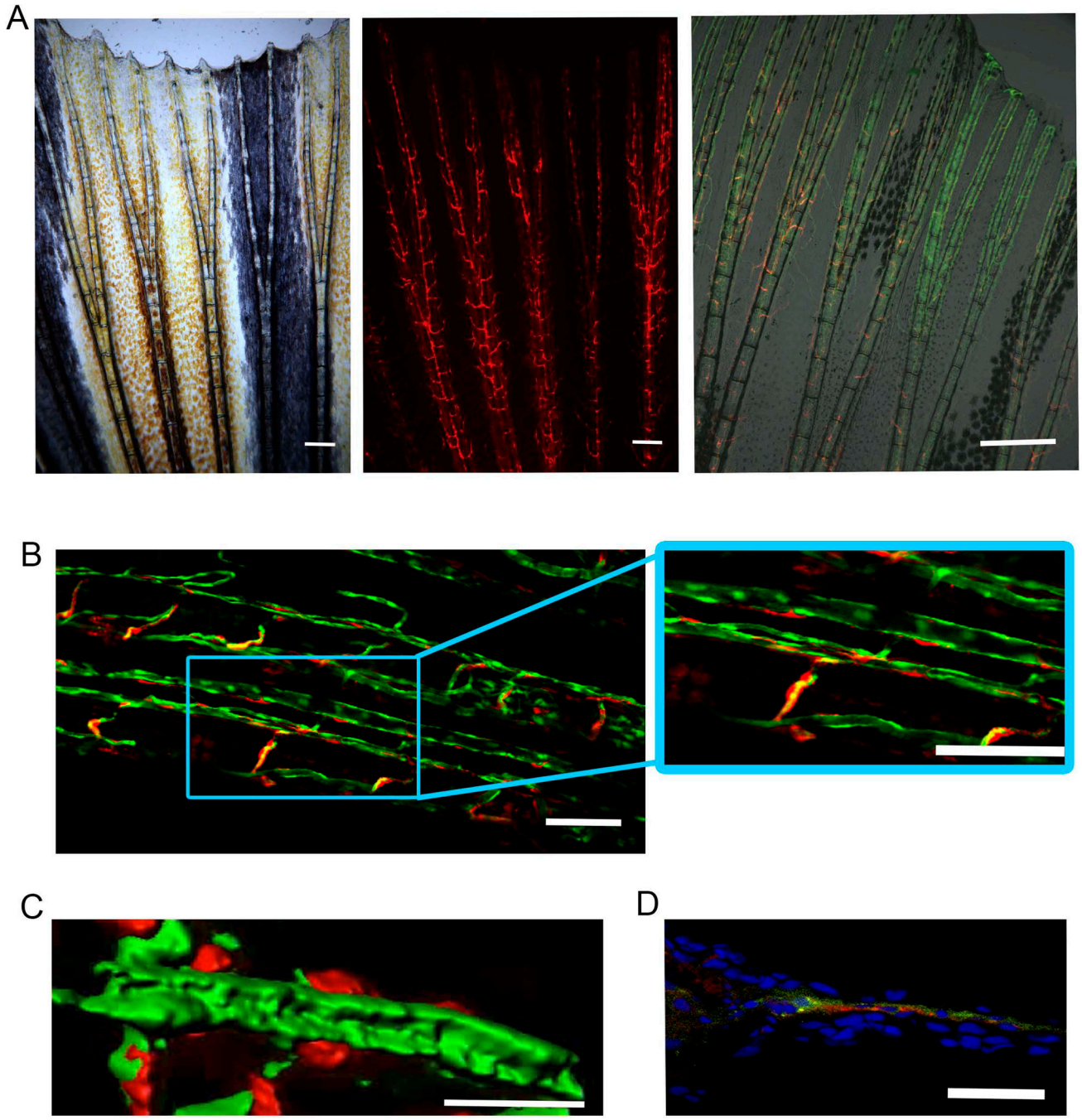

Figure 1.

The *sdf1a:DsRed* transgene illuminates perivascular cells. (A) Caudal fin of 10-week old *sdf1a:DsRed* zebrafish at 5×. Scale bar represents 200 microns. Rightmost panel shows live fluorescent microscopy of the tail-fin in a 10-week old *fli1:EGFP* crossed to *sdf1a:DsRed* shows a population of *sdf1a*^{DsRed} cells as perivascular in anatomical location. Scale bar represents 500 microns. (B) Confocal microscopy of a caudal tail fin from a *fli1:EGFP* × *sdf1a:DsRed* transgenic zebrafish shows enhanced discrimination of *sdf1*^{DsRed} cells. Scale bars represent 50 microns. (C) Live confocal microscopy of perivascular cells followed by

3D surface rendering of a z-stack using the Zeiss Zen software. Scale bar represents 20 microns. (D) Immunohistochemistry of *fli1:EGFP* × *sdf1a:DsRed* caudal tail fin cross-section. Co-staining was performed with anti-EPG-FITC and anti-DsRed primary antibodies. Anti-DsRed detection was performed using a secondary antibody, donkey anti-rabbit-Cy3. Scale bar represents 50 microns.

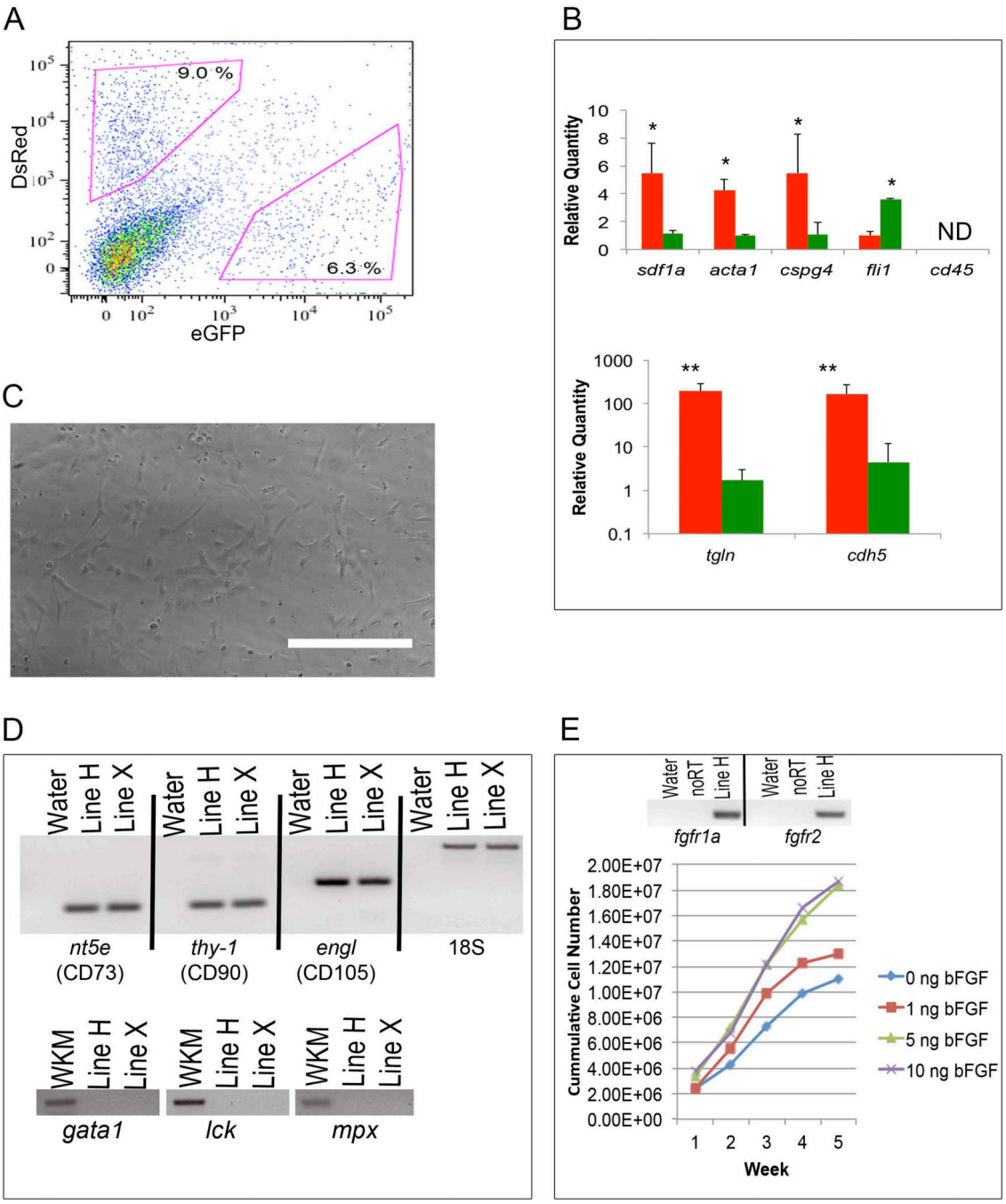

Figure 2.

Perivascular *sdf1a*^{DsRed} cells express markers of perivascular cells and can be cultured-expanded. (A) The caudal tail fins of adult *fli1:EGFP* × *sdf1a:DsRed* animals (n = 8 – 12) were amputated and treated with collagenase to produce a single cell suspension. Shown is a representative scatter plot of green *fli1*^{EGFP} endothelial cells and *sdf1a*^{DsRed} perivascular cells. (B) The *fli1*^{EGFP} endothelial cells and *sdf1a*^{DsRed} perivascular cells were sorted by flow cytometry and RNA isolated for qRT-PCR. N = 3 experiments, * and ** represent $p < 0.05$ and $p < 0.01$ respectively from a Student's t-test. ND, not detected. (C) Phase-contrast

microscopy of culture-expanded perivascular *sdf1a*^{DsRed} cells 6 weeks after primary isolation. Scale bar represent 100 microns. (D) RNA was extracted from cultured *sdf1a*^{DsRed} cells and RT-PCR performed for MSC and hematopoietic markers. Shown are the zebrafish gene names as well as the human cluster of differentiation (CD) designations. Whole kidney marrow (WKM) cells were used as a positive control. (E) RT-PCR showing FGF-family gene receptor expression and cumulative *sdf1a*^{DsRed} cell counts cultured in increasing amounts of bFGF.

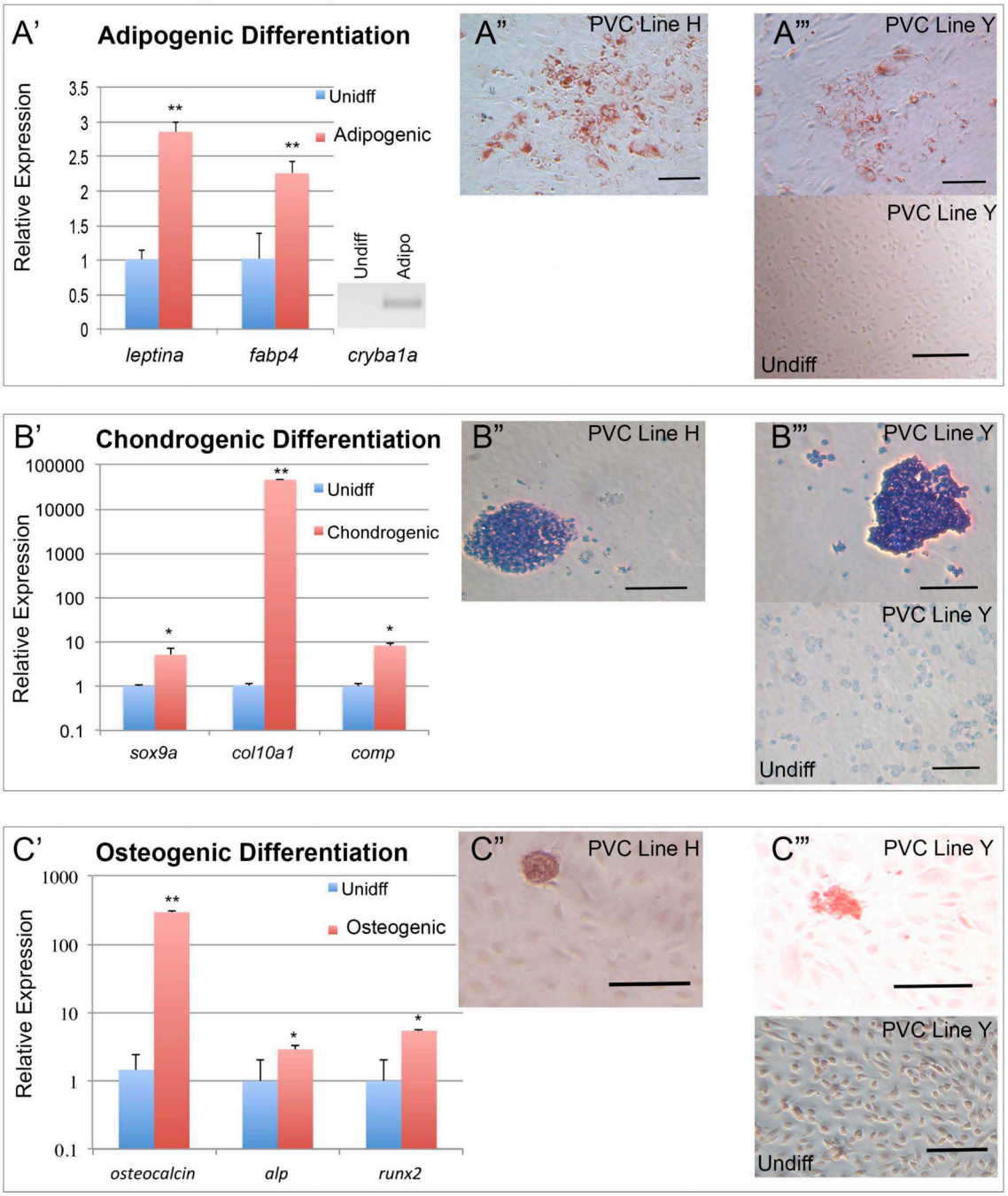

Figure 3.

Differentiation of cultured *sdf1a*^{DsRed} cells into mesodermal lineages. (A'–C') Cells were cultured in adipogenic, chondrogenic, or osteogenic promoting media for 4 weeks. Relative gene expression was determined by qRT-PCT and $\Delta\Delta C_T$ calculation relative to undifferentiated cells as shown. N = 3 experiments, * and ** represent $p < 0.05$ and $p < 0.01$ respectively from a Student's t-test. (A"–C") Show examples of PVC line H differentiated and stained Oil-Red-O, toluidine blue, or Alizarin red to indicate adipogenic, chondrogenic, and osteogenic cells respectively. (A"' – C"') Show examples of PVC line Y differentiated

and undifferentiated followed by staining with Oil-Red-O, toluidine blue, or Alizarin red to indicate adipogenic, chondrogenic, and osteogenic cells respectively. Scale bars represents 100 microns in adipogenic and osteogenic images and 500 microns in chondrogenic images.

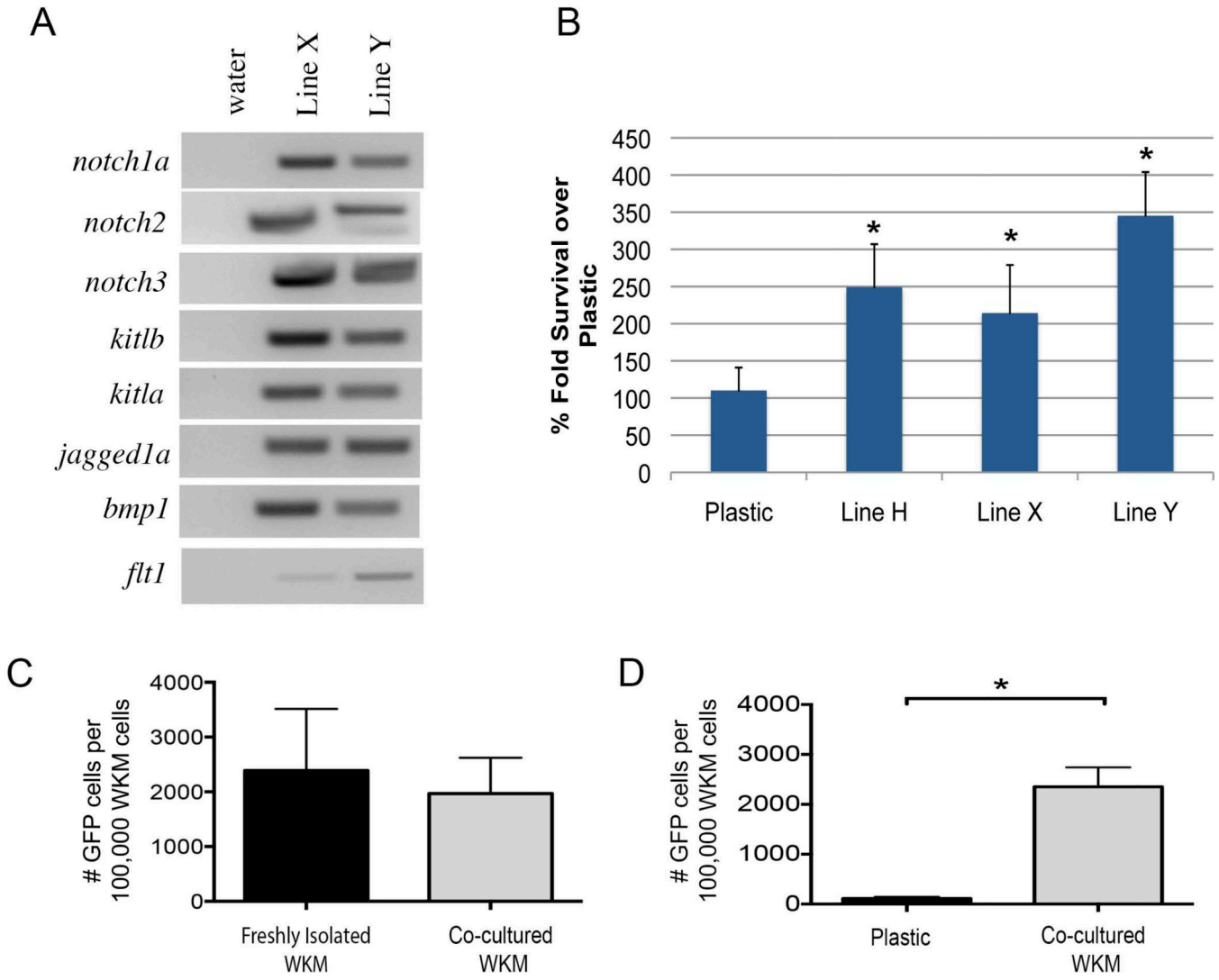

Figure 4.

Cultured *sdf1a*^{DsRed} cells support engraftable hematopoietic cells. (A) Genes known to be important for the maintenance of hematopoietic cells were amplified by RT-PCR. Shown are the results from two of three *sdf1a*^{DsRed} cell lines. (B) 50,000 WKM from *bactin2:GFP* fish were co-cultured on a monolayer of *sdf1a*^{DsRed} cells (lines H, X, Y) for 16 days followed by enumeration using a flow cytometry and counting beads (n = 15/group). * indicates p-value < 0.001 from a Student's t-test. (C) Two days after 20 Gy irradiation, wild-type zebrafish were transplanted with 50,000 *bactin2:GFP* WKM from freshly isolated donors or previously co-cultured with *sdf1a*^{DsRed} PVC from Line H. Engraftment analysis was performed 7 days after transplant by flow cytometry for GFP (n = 5 – 7 animals/group). Student's t-test showed no significant difference between the groups (p = 0.65). (D) WKM from *bactin2:GFP* transgenics was co-cultured with *sdf1a*^{DsRed} PVC cells from Line H for 16 days versus cells on plastic alone. The entire contents of a well were used for transplant as above and engraftment determined at seven days post transplant (n = 10 – 12 animals/group). * indicates p-value < 0.001 from a Student's t-test.

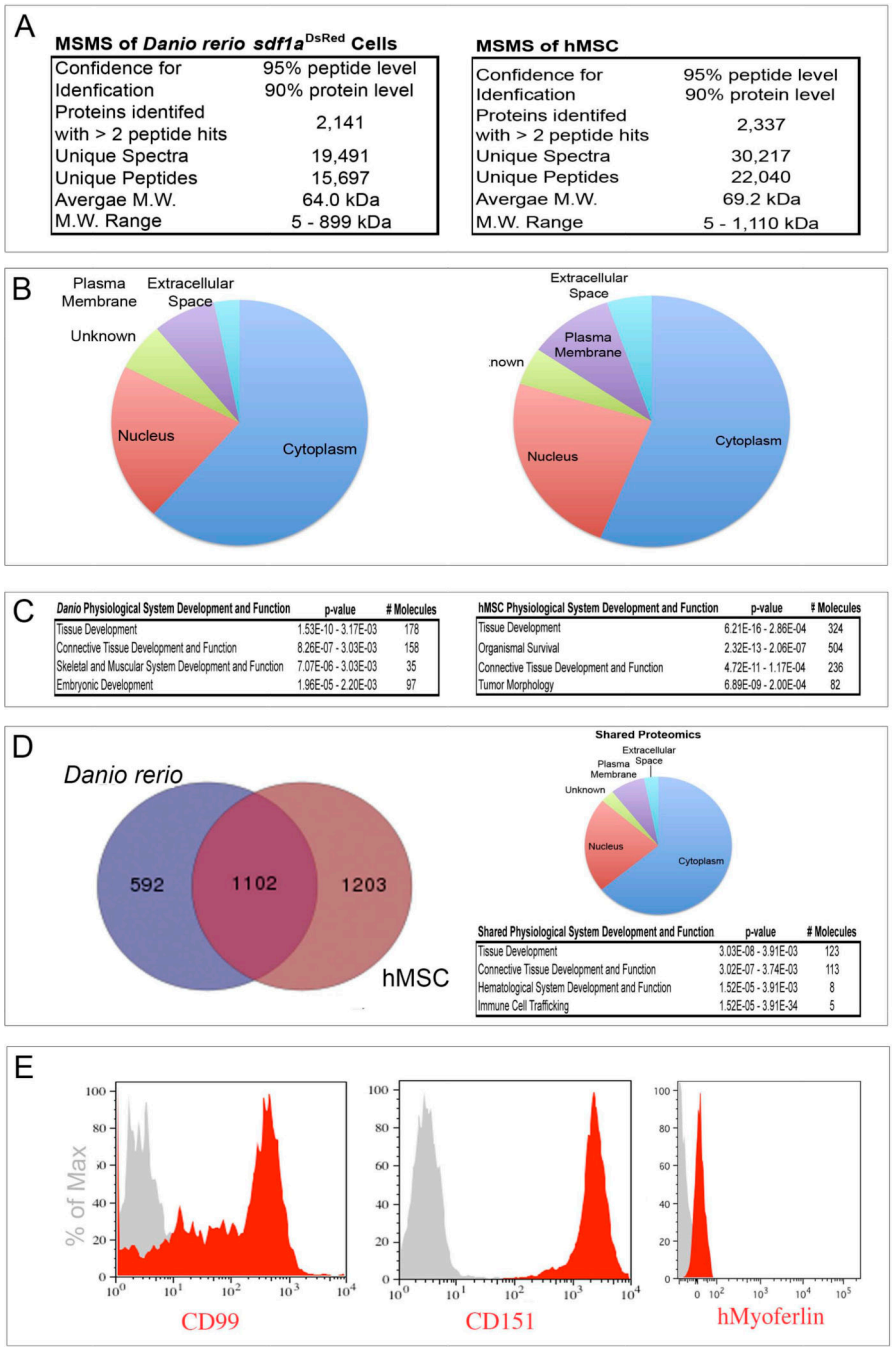

Figure 5.

Proteomics of cultured *sdf1a*^{DsRed} cells and hMSC. Whole cell lysates were prepared and subjected to 2-dimensional liquid chromatography as described in the supplemental methods. Tandem mass spectrometry was then used to identify peptides on a capillary LC-nanoESI-Orbitrap XL mass spectrometer. Peptide matching to full-length proteins was performed using Sequest (version 27, rev. 12). (A) Absolute numbers of spectra, peptides, and proteins identified. (B) Results of IPA® analysis showing distribution of proteins by cellular compartment. (C) IPA® analysis showing top hits in the “Physiological System and

Development" category. (D) Venn diagram showing common proteins identified between cultured *sdf1a*^{DsRed} cells and hMSC, their cellular compartment, and IPA analysis showing top hits in the "Physiological System and Development" category. (E) Flow cytometry histograms of hMSC for three novel proteins identified in both cultured *sdf1a*^{DsRed} cells and hMSC. Grey histograms show the isotope control antibody.

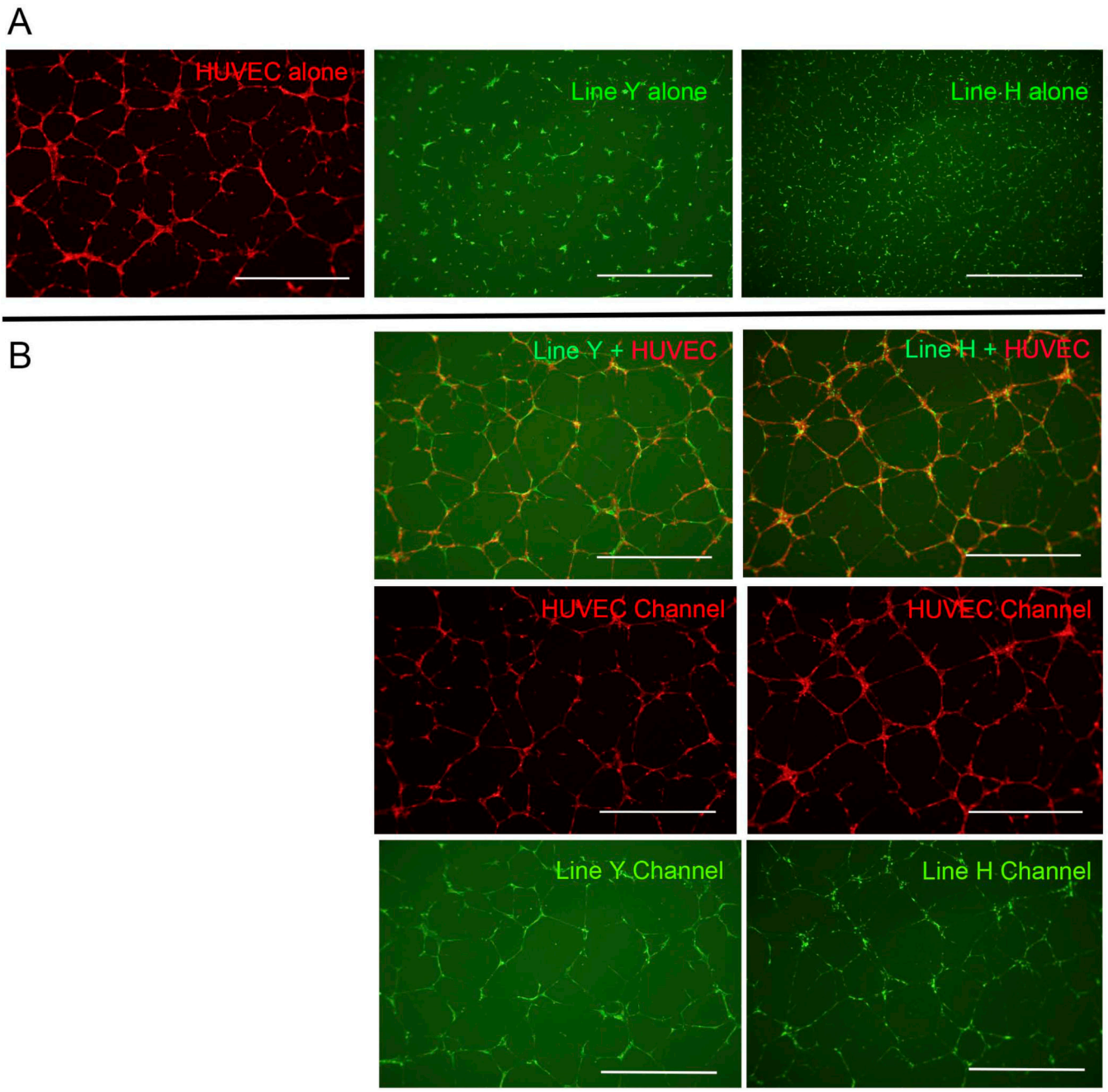

Figure 6.

Co-culture of *sdf1a*^{DsRed} cells with HUVECs shows vascular branching. 15,000 HUVECs were labeled with CellTracker™ Orange and 10,000 cultured *sdf1a*^{DsRed} cells were labeled with CellTracker™ Green. Cells were placed atop 100 μL of matrigel in a 96-well plate in the presence of EGM-2 media for 10 – 16 hours prior to imaging. (A) HUVECs and two *sdf1a*^{DsRed} cell lines cultured alone. (B) Co-culture of HUVECs with *sdf1a*^{DsRed} cells and imaged under the appropriate filters. Scale bars represent 1000 microns.

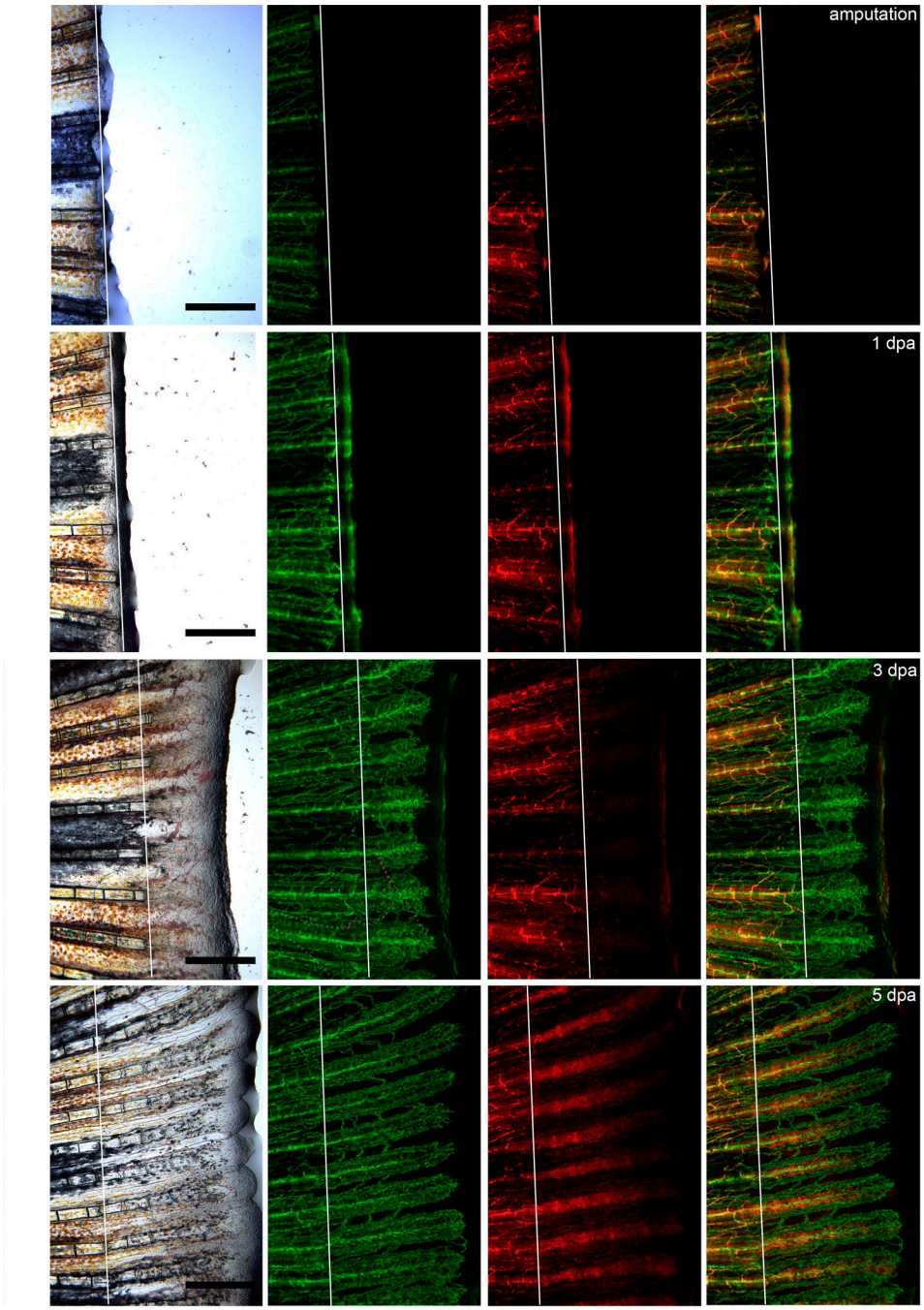

Figure 7.

The contribution of *sdf1a*$^{\text{DsRed}}$ cells to fin regeneration. The caudal tail of *sdf1a*$^{\text{DsRed}}$ × *fli1:EGFP* double transgenic was amputated on day 0 (amputation plane indicated by the white line). The same animal was anaesthetized and imaged using the appropriate filters at the time points given. Photos are representative of the same regeneration experiment performed in ten animals. Scale bars represent 100 microns.